J. Plasma Physics (1994), *vol.* 52, *part* 1, *pp.* 23–42

Copyright © 1994 Cambridge University Press

Magnetohydrodynamic instability driven by cosmic rays

By CHUNG-MING KO AND AN-TZONG JENG

Department of Physics and Institute of Astronomy, National Central University,
Chung-Li, Taiwan, Republic of China

(Received 11 April 1994)

Magneto-acoustic instability driven by cosmic rays and the waves that they excite was first studied by McKenzie and Webb and by Zank. In the present paper this instability is reconsidered. In general, the cosmic-ray plasma system is unstable. However, depending on how the time scale is chosen, the results and interpretation may be different from those of McKenzie and Webb and of Zank, particularly in the long- and short-wavelength limits. To illustrate this instability in an astrophysical context, we take our Galaxy and supernova remnants as examples. In those examples, length scales shorter than 2·5 kpc and 1·5 pc respectively are susceptible to this instability, and the growth times are of the order of 4×10^8 and $1{\cdot}5 \times 10^4$ yr respectively.

1. Introduction

A common consensus about the interstellar medium (ISM) in our Galaxy is that the energy densities of various components, including thermal plasmas, turbulent plasmas, magnetic fields and cosmic rays, are roughly the same. Thus cosmic rays, which couple to thermal plasmas via embedded magnetic fields, play a dynamical role in various astrophysical objects. For example, study of cosmic-ray-modified shocks (see e.g. Drury & Völk 1981; Axford, Leer & McKenzie 1982; McKenzie & Völk 1982; Webb 1983; Duffy 1992) enables us to estimate the efficiency of shock acceleration of cosmic rays. A shock in a supernova remnant will accelerate cosmic rays, leading to modification of the shock, and hence affecting the evolution of the remnant (see e.g. Drury, Markiewicz & Völk 1989; Jones & Kang 1992). Modification of the solar wind termination shock by galactic cosmic rays or anomalous components has a direct effect on cosmic-ray modulation (see e.g. Ko, Jokipii & Webb 1988; Lee & Axford 1988; Ko 1991*b*). Cosmic rays, regarded as an extremely hot tenuous gas, can support a galactic halo or drive a galactic wind (see e.g. Hartquist & Morfill 1986; Ko, Dougherty & McKenzie 1991; Ko 1991*a*; Ipavich 1975; Zank 1989*b*; Breitschwerdt, McKenzie & Völk 1991, 1993). All of these phenomena illustrate how cosmic rays are dynamically important in determining the structure of the ISM and the Galaxy.

In this paper we discuss another aspect of the cosmic-ray–plasma system. We re-visit the work of McKenzie & Webb (1984) and Zank (1989*a*) on cosmic-ray-driven magneto-acoustic instability. They considered a homogeneous or uniform system, which we may call a unidirectional wave system. In detail, the system comprises a thermal plasma in which a magnetic field is embedded, cosmic rays and an Alfvén wave field propagating along the magnetic field. The wave field contains pre-existing and self-excited waves (those excited by cosmic-ray streaming instability). The plasma, cosmic rays and Alfvén waves are all regarded as fluids. A general conclusion is that the slow magneto-acoustic mode can be driven unstable when there is diffusion of cosmic rays. The energy feeding the instability comes from cosmic rays through the *frictional* force in generating Alfvén waves (for a detailed discussion see McKenzie & Webb 1984). In this work we consider a similar system to that in McKenzie & Webb (1984) and Zank (1989*a*), except that we take a wave-pressure-dependent cosmic-ray diffusion coefficient. Moreover, we allow for perturbation of the oppositely propagating wave. We confirm that in the linear regime the system is unstable in general, and show that only a single slow magneto-acoustic mode is unstable. (However, we find a new stable '*island*', a set of measure zero in parameter space.) To further understand this unstable mode, we numerically investigate the relation between its growth rate and various parameters, which may give, say, the most unstable length scale.

The hydrodynamic model for the cosmic-ray–plasma system with two Alfvén wave fields is presented in §2. A linear stability analysis is performed in §3, where we also analyse some asymptotic configurations, and show that the slower of the slow magneto-acoustic modes is unstable. Section 4 provides a detailed parametric study of the growth rate of the single unstable slow mode. A summary and a discussion of possible astrophysical manifestations of this instability is given in §5.

2. The model

The following hydrodynamic model describes, in a self-consistent manner, the interactions between a magnetized thermal plasma, cosmic rays and turbulent Alfvén waves. The Alfvén waves generated by cosmic-ray streaming instability act like a 'clutch' between the magnetized thermal plasma and cosmic rays. The model also includes the second-order Fermi effect. The governing equations are the ideal magnetohydrodynamic (MHD) equations augmented by energy equations for the cosmic rays and Alfvén waves (Ko 1992; see also Drury & Völk 1981; McKenzie & Völk 1982). The overall mass continuity equation is simply that for the thermal plasma (since the cosmic rays and Alfvén waves are assumed to be massless fluids):

$$\frac{\partial \rho}{\partial t}+\nabla.(\rho \mathbf{U}) = 0, \tag{1}$$

where ρ and $\mathbf{U}$ are the density and flow velocity of the plasma. The overall momentum equation is

$$\rho\frac{\partial \mathbf{U}}{\partial t}+\rho(\mathbf{U}.\nabla)\mathbf{U} = -\nabla(P_g+P_c+P_w^+ + P_w^-)+\mathbf{J}\times\mathbf{B}+\rho\mathbf{g}. \tag{2}$$

Here P_g, P_c and $P_w^\pm$ are the pressures of the thermal plasma, cosmic rays, and forward- and backward-propagating waves respectively. $\mathbf{B}$ is the background magnetic field and $\mathbf{J}$ is the current density, and in the MHD approximation $\mathbf{J} = (\nabla\times\mathbf{B})/\mu_0$ (with μ_0 the magnetic permeability of the vacuum). $\mathbf{g}$ is some external acceleration (e.g. gravitation). The energy equations of the thermal plasma, cosmic rays, waves and background magnetic field are

$$\frac{\partial E_g}{\partial t}+\nabla.\mathscr{F}_g=-\mathbf{U}.\nabla(P_c+P_w^+ +P_w^-)+\mathbf{J}.\mathbf{E}+\rho\mathbf{U}.\mathbf{g}, \tag{3}$$

$$\frac{\partial E_c}{\partial t}+\nabla.\mathscr{F}_c=\left(\mathbf{U}+\frac{\nu_+-\nu_-}{\nu_++\nu_-}\mathbf{V}_A\right).\nabla P_c+\frac{P_c}{\tau}, \tag{4}$$

$$\frac{\partial E_w^\pm}{\partial t}+\nabla.\mathscr{F}_w^\pm=\mathbf{U}.\nabla P_w^\pm \mp\frac{\nu_\pm}{\nu_++\nu_-}\mathbf{V}_A.\nabla P_c-\frac{P_c}{2\tau}, \tag{5}$$

$$\frac{\partial E_B}{\partial t}+\nabla.\mathbf{S}=-\mathbf{J}.\mathbf{E}. \tag{6}$$

Here

$$V_A=\frac{\mathbf{B}}{(\mu_0\rho)^{\frac{1}{2}}}, \tag{7}$$

and the energy densities and fluxes are given by

$$\left.\begin{aligned}
&E_g=\tfrac{1}{2}\rho U^2+\rho\varepsilon=\tfrac{1}{2}\rho U^2+\frac{P_g}{\gamma_g-1},\\
&E_c=\frac{P_c}{\gamma_c-1},\quad E_w^\pm=2P_w^\pm,\quad E_B=\frac{B^2}{2\mu_0}
\end{aligned}\right\} \tag{8}$$

and

$$\left.\begin{aligned}
&\mathscr{F}_g=\mathbf{U}(\tfrac{1}{2}\rho U^2+\rho\varepsilon+P_g),\\
&\mathscr{F}_c=\left(\mathbf{U}+\frac{\nu_+-\nu_-}{\nu_++\nu_-}\mathbf{V}_A\right)(E_c+P_c)-\boldsymbol{\kappa}.\nabla E_c,\\
&\mathscr{F}_w^\pm=(\mathbf{U}\pm\mathbf{V}_A)E_w^\pm+\mathbf{U}P_w^\pm,\\
&\mathbf{S}=\frac{1}{\mu_0}\mathbf{E}\times\mathbf{B},
\end{aligned}\right\} \tag{9}$$

where $\nu_\pm$ are the collisional frequencies of cosmic rays scattered by forward- and backward-propagating waves, and ε is the internal energy per unit mass of the plasma. In ideal MHD the electric field $\mathbf{E}=-\mathbf{U}\times\mathbf{B}$. The derivation of the cosmic-ray and wave energy equations (4) and (5) can be found in Ko (1992). (Note that the right-hand side of equation (28) of Ko (1992) lacks the term $\mathbf{J}.\mathbf{E}$, and a factor of $\frac{1}{3}$ should be added to the right-hand side of equation (14) of that paper.)

The set of equations is completed by Faraday's induction equation, which in the MHD approximation can be written as

$$\frac{\partial\mathbf{B}}{\partial t}=\nabla\times(\mathbf{U}\times\mathbf{B}), \tag{10}$$

along with the omnipresent constraint equation

$$\nabla . \mathbf{B} = 0. \tag{11}$$

It is clear from the energy equations (3)–(5) that energy exchange between thermal plasma, cosmic rays and waves is facilitated by two processes: the power of different pressure gradients ($\mathbf{V}_A . \nabla P_c, \mathbf{U} . \nabla P_c$ and $\mathbf{U} . \nabla P_w^{\pm}$), and the second-order Fermi effect (P_c/τ). A detail discussion of this model can be found in McKenzie & Webb (1984) (without second-order Fermi effect) and Ko (1992) (with second-order Fermi effect).

To fix ideas, consider the cosmic rays as ultra-relativistic particles, with no cross-field-line diffusion. The diffusion tensor $\boldsymbol{\kappa}$ and the growth time of the second-order Fermi effect τ are then given by (Ko 1992)

$$\boldsymbol{\kappa} = \frac{c^2}{3(\nu_+ + \nu_-)} \frac{\mathbf{V}_A \mathbf{V}_A}{V_A^2}, \quad \frac{1}{\tau} = 16 \frac{\nu_+ \nu_-}{\nu_+ + \nu_-} \frac{V_A^2}{c^2}. \tag{12}$$

We take simple polytropic relations for the thermal plasma and cosmic rays (see (8)), in which γ_g and γ_c are constants. For ultra-relativistic cosmic rays $\gamma_c = \frac{4}{3}$. Moreover, we assume that the collisional frequencies are proportional to the Alfvén-wave pressures, i.e. $\nu_{\pm} = \alpha P_w^{\pm}$ (i.e. α represents the coupling between cosmic rays and plasma).

Ignoring the spatial structure of the system (or considering a very localized spatial region), it can be shown that the second-order Fermi effect drives the system to a unidirectional wave system (Ko 1992). This essentially means that after a while only one of the waves survives. Now, let us turn on some spatial perturbation and ask what will happen. In the following sections we show that only in a set of measure zero in parameter space is the system stable or marginally stable.

3. Linear stability analysis

One of the first questions one would like to ask about a system like that described in §2 regards the nature of the simple equilibrium state and its stability. If the second-order Fermi effect or an external force is present, a simple uniform state (where state variables are independent of time and space) will not exist in the above system, (1)–(6), unless either forward- or backward-propagating wave vanish (see (12)) and $\mathbf{g} = 0$. In a uniform state the absolute value of the plasma velocity is irrelevant, because the model is invariant under Galilean transformations. In this work we focus on uniform equilibrium states. Without loss of generality, we take the unperturbed plasma velocity and forward-propagating Alfvén-wave pressure to be zero (cf. McKenzie & Webb 1984; Zank 1989*a*). On the unperturbed uniform state $\psi_0 = (\rho_0, \mathbf{U}_0, P_{g0}, P_{c0}, P_{w0}^{\pm}, \mathbf{B}_0)$ (with $\mathbf{U}_0 = 0$ and $P_{w0}^{+} = 0$), we introduce a small perturbation $\delta\psi = (\delta\rho, \delta\mathbf{U}, \delta P_g, \delta P_c, \delta P_w^{\pm}, \delta\mathbf{B})$. After linearization, the relevant equations for the perturbation are as listed in appendix A with $\mathbf{U}_0 = 0$, $P_{w0}^{+} = 0$ and $\mathbf{g} = 0$. To proceed, we make use of plane-wave perturbations (i.e. Fourier analysis) such as $\delta\psi \propto \exp[i(\mathbf{k} . \mathbf{x} - \omega t)]$, where $\mathbf{k}$ is real and ω may be complex. The system has two natural directions, $\mathbf{B}$ and $\mathbf{k}$, and this leads to two distinct cases. In one $\mathbf{B}$ and $\mathbf{k}$ are parallel to each other while in the other they are not. However, after some manipulation, the two cases give the same dispersion relation, which can be written as

$$\begin{aligned}0 = k^{11} V_p^2\left(V_p-\mu V_{A0}+i\frac{4V_{A0}P_{c0}}{3P_{w0}^-}\right)(V_p^2-\mu^2 V_{A0}^2)^2 \\ \times (V_p+\mu V_{A0})(V_p+\mu V_{A0}+i\eta\mu^2 V_{A0}) \\ \times\left[V_p^2-V_{A0}^2\frac{V_p^2(1-\mu^2)}{V_p^2-\mu^2 V_{A0}^2}-\alpha_{s0}^2-a_{w0}^{-2}\frac{V_p+\frac{1}{3}\mu V_{A0}}{V_p+\mu V_{A0}}\right. \\ \left.-a_{c0}^2\frac{(V_p+\frac{1}{2}\mu V_{A0})^2}{(V_p+\mu V_{A0})(V_p+\mu V_{A0}+i\eta\mu^2 V_{A0})}\right],\end{aligned} \tag{13}$$

in which the phase speed of the plane-wave perturbation and the 'sound' speeds of thermal plasma, cosmic rays and waves are given by

$$V_p = \frac{\omega}{k}, \quad a_{s0}^2 = \frac{\gamma_g P_{g0}}{\rho_0}, \quad a_{c0}^2 = \frac{\gamma_c P_{c0}}{\rho_0}, \quad a_{w0}^{-2} = \frac{3P_{w0}^-}{2\rho_0} \tag{14}$$

respectively, μ is the cosine of the angle between $\mathbf{B}$ and $\mathbf{k}$ (i.e. $\mu = \mathbf{V}_{A0}\cdot\mathbf{k}/V_{A0}k$), and η is the normalized cosmic-ray diffusion coefficient, defined as

$$\eta \equiv kl_D, \quad l_D \equiv \frac{c^2}{3\alpha P_{w0}^- V_{A0}}. \tag{15}$$

We call l_D the *diffusion length scale*, and $1/\eta$ may be considered as the normalized coupling strength.

As expected, the dispersion relation (13) includes that of ideal MHD. The terms in the second set of parentheses represent the Alfvén mode, and those in the square brackets (with $a_{c0} = a_{w0}^- = 0$, i.e. cosmic rays and waves are absent) represent the magneto-acoustic mode. The terms in the first set of parentheses represent the decaying mode of forward-propagating waves. (Of course, if we consider at the outset the unperturbed background to contain forward-propagating waves instead of backward-propagating ones, the decaying mode will then be that of the backward-propagating waves.) In the following we concentrate on the terms in the square brackets, and indeed we show that this compressive mode is unstable almost everywhere in parameter space. (This mode is shown to be compressive in appendix B. See also McKenzie & Webb (1984).)

As one can imagine, it is not easy to thoroughly analyse the terms in the square brackets in (13), which involve six parameters (V_{A0}, a_{s0}, a_{w0}^-, a_{c0}, μ and η). Nevertheless, one may proceed by studying some asymptotic configurations. We shall present four cases later. In any case, we know that the square bracketted expression has five roots (i.e. five modes) in general. McKenzie & Webb (1984) showed that the system is 'stable' in the short-wavelength limit ($\eta \rightarrow \infty$). They also showed that in the long-wavelength limit ($\eta = 0$) the system is 'unstable' if a_{s0} is sufficiently large. However, we must be very careful about the way in which they used terms 'stable' and 'unstable'. What they (see also Zank 1989*a*) mean is that the imaginary part of the perturbation phase speed is zero in the short-wavelength limit, and is positive in the long-wavelength limit together with sufficiently large plasma pressure. A mode is unstable (stable) if and only if Im $(\omega) > 0(\leqslant 0)$. Therefore, even if Im $(V_p) > 0$, the system might be marginally stable (Im $(\omega) = 0$) in the long-wavelength limit $(k = 0)$. On the other hand, even if Im $(V_p) = 0$, the system might be unstable (Im $(\omega) > 0$) in the short-wavelength limit $(k \rightarrow \infty)$. η is a measure of the coupling between the plasma and cosmic rays. It depends on k and P^-_{w0}. If we take k as constant (i.e. we consider a particular wavelength of perturbation), we find that the system is unconditionally stable when $\eta = 0$ $(P^-_{w0} \rightarrow \infty)$ and when $\eta \rightarrow \infty$ $(P^-_{w0} = 0)$. If we take P^-_{w0} as a constant (i.e. we consider a fixed diffusion length l_D), we find that the system is unconditionally stable when $\eta = 0$ (i.e. $k = 0$), but unstable when η (i.e. k) is infinite (see §4 for details). Furthermore, we find that the system is stable (or marginally stable) under a combination of μ, V_{A0}, a_{s0} and a^-_{w0}. When

$$a^2_{s0} = \tfrac{1}{3}(1 - \tfrac{1}{4}\mu^2)\, V^2_{A0} + \tfrac{1}{3}(a^-_{w0})^2, \tag{16}$$

one of the five roots of the square bracketted expression in (13) is $V_p = -\frac{1}{2}\mu V_{A0}$, which says that this mode is marginally stable. The remaining four roots can be shown to have negative imaginary part (see appendix C), i.e. all modes are stable. Finally, there is an extra stable region, which is a consequence of the assumption of the absence of cross-field-line diffusion in our model. This region is $\mu = 0$ (or the perturbation wave vector is perpendicular to the magnetic field). Indeed, the square of the phase speed is just the sum of the square of the 'sound' speeds $(V^2_p = V^2_{A0} + a^2_{s0} + (a^-_{w0})^2 + a^2_{c0})$. We believe that the system is stable only within these three (or four) regions of the parameter space, and they span a set of measure zero only.

We now justify our assertion by presenting four asymptotic configurations: (i) small a_{c0}; (ii) large η; (iii) small η; and (iv) a small deviation from the condition (16). Except that we are able to spell out which is the unstable mode, the result of the first three asymptotic analyses are basically the same as those of Zank (1989*a*). For these first three cases we let

$$V_p = V^{(0)}_p + \epsilon V^{(1)}_p + O(\epsilon^2), \tag{17}$$

where $\epsilon = a^2_{c0}$, $1/\eta$ and η for cases (i), (ii) and (iii) respectively. Substituting (17) into the square brackets of (13), we find that $V^{(0)}_p$ satisfies $\mathscr{F}(V_p) = 0$ for cases (i) and (ii), and $\mathscr{G}(V_p) = 0$ for case (iii), where

$$\mathscr{F}(V_p) \equiv V^2_{A0} \frac{V^2_p(1-\mu^2)}{V^2_p - \mu^2 V^2_{A0}} - V^2_p + a^2_{s0} + a^{-2}_{w0} \frac{V_p + \frac{1}{3}\mu V_{A0}}{V_p + \mu V_{A0}}, \tag{18}$$

$$\mathscr{G}(V_p) \equiv \mathscr{F}(V_p) + a^2_{c0} \frac{(V_p + \frac{1}{2}\mu V_{A0})^2}{(V_p + \mu V_{A0})^2}. \tag{19}$$

The first-order term is given by

$$V^{(1)}_p = \frac{(V^{(0)}_p + \frac{1}{2}\mu V_{A0})^2[-1 + i\,\eta\mu^2\, V_{A0}/(V^{(0)}_p + \mu V_{A0})]}{[(V^{(0)}_p + \mu V_{A0})^2 + (\eta\mu^2\, V_{A0})^2]\, d\mathscr{F}/dV_p|_{V^{(0)}_p}} \tag{20}$$

for case (i),

$$V^{(1)}_p = i a^2_{c0} \frac{(V^{(0)}_p + \frac{1}{2}\mu V_{A0})^2}{\mu^2\, V_{A0}(V^{(0)}_p + \mu V_{A0})} \Bigg/ \frac{d\mathscr{F}}{dV_p}\bigg|_{V^{(0)}_p} \tag{21}$$

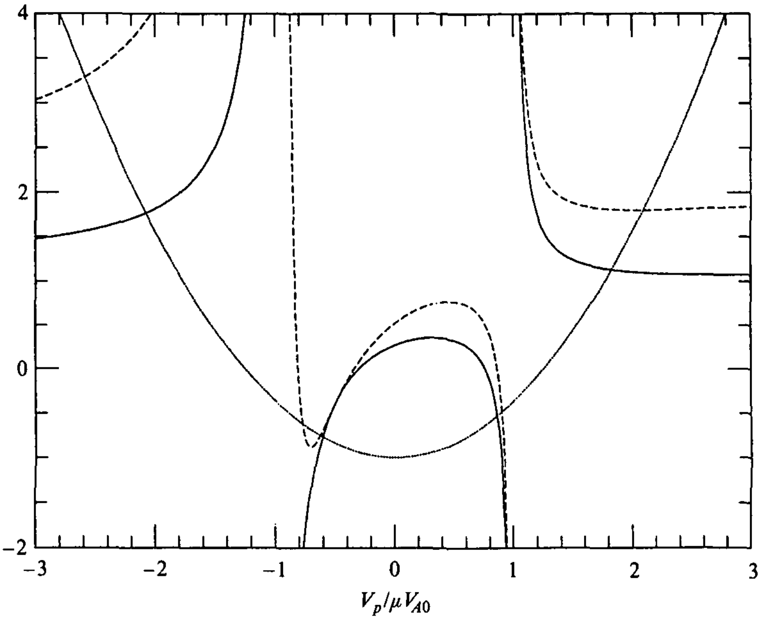

FIGURE 1. Graphical solution of (18) and (19) (different zeroth-order dispersion relations). The solid, dashed and dotted lines correspond to the functions $\mathscr{F}(V_p)+V_p^2-a_{s0}^2$, $\mathscr{G}(V_p)+V_p^2-a_{s0}^2$ and $V_p^2-a_{s0}^2$ respectively. The figure clearly shows that $\mathscr{G}(V_p)$ may have three or five real roots while $\mathscr{F}(V_p)$ has four real roots. In this example $a_{s0}=a_{c0}=V_{A0}$, $a_{w0}^-=2V_{A0}/5^{\frac{1}{2}}$ and $\mu=0{\cdot}8$.

for case (ii) and

$$V_p^{(1)} = ia_{c0}^2\frac{\mu^2 V_{A0}(V_p^{(0)}+\frac{1}{2}\mu V_{A0})^2}{(V_p^{(0)}+\mu V_{A0})^3}\Big/\left.\frac{d\mathscr{G}}{dV_p}\right|_{V_p^{(0)}} \tag{22}$$

for case (iii). In figure 1 the solid, dashed and dotted lines correspond to the functions $\mathscr{F}(V_p)+V_p^2-a_{s0}^2$, $\mathscr{G}(V_p)+V_p^2-a_{s0}^2$ and $V_p^2-a_{s0}^2$ respectively. The intersections of the dotted and solid lines give the real roots of $\mathscr{F}(V_p)=0$, while the intersections of the dotted and dashed lines give those of $\mathscr{G}(V_p)=0$. Consider case (iii). By moving the dotted line up and down in figure 1 (which corresponds to changing a_{s0}^2), we observe that $\mathscr{G}$ may have three or five real roots. In the case of five real roots, it is clear from the location of the roots and the derivative of $\mathscr{G}$ at them that only one of the five $V_p^{(1)}$ has positive imaginary part. In fact, this is the slower of the backward-propagating slow magneto-acoustic modes. In the case of three real roots the remaining two roots are complex conjugates (with real parts lying between 0 and $-\mu V_{A0}$, i.e. the backward-propagating slow magneto-acoustic modes). Although one of these two modes has Im $(V_p^{(0)})>0$, they are marginally stable because the zeroth-order growth rate vanishes when either k or P_{w0}^- is kept fixed (see the discussion above (16)). However, when we go to first order, the corresponding two Im $(V_p^{(1)})$ are complex conjugates. Im $(V_p^{(1)})$ is negative for the other three modes (the same argument applies as in the case of five real roots). Hence *one* and *only one* of the modes is unstable. Now consider cases (i) and (ii). Figure 1 shows that $\mathscr{F}$ has four real roots. Similarly to case (iii), the location of the roots and the derivative of $\mathscr{F}$ at them show that Im $(V_p^{(1)})>0$ for one of the modes only. This is also the backward-propagating slow magneto-acoustic mode. We should point out that the fifth mode of case (i) or (ii) is stable. In fact, in case (i) this mode is $V_p = -\mu V_{A0} - i\eta\mu^2 V_{A0} + O(a_{c0}^2)$, while in case (ii) it is $V_p = -i\eta\mu^2 V_{A0} - \mu V_{A0} + O(1/\eta)$.

The fourth asymptotic case stems from the condition (16). For fixed μ and V_{A0}, we consider a plane surface parallel to and at a small distance ϵV_{A0} from the surface defined by (16). As mentioned above, the system is stable when (16) is satisfied. Since we are only interested in the stability of the system in the neighbourhood of (16), it is sufficient to investigate the marginally stable mode, $V_p = -\frac{1}{2}\mu V_{A0}$ (the remaining four modes are stable, since they all have negative imaginary parts). After some manipulation, we obtain

$$V_p = -\tfrac{1}{2}\mu V_{A0} - \epsilon \frac{10^{\frac{1}{2}}15\,\mu V_{A0}}{4\mathscr{M}} + \epsilon^2 \frac{75\mu V_{A0}}{32\mathscr{M}^3}\left[\mathscr{N} + 2700\frac{a_{c0}^2(-1+2i\eta\mu)}{V_{A0}^2(1+4\eta^2\mu^2)}\right] + O(\epsilon^3), \tag{23}$$

where

$$\left.\begin{aligned} \mathscr{M} &= \{9[V_{A0}^2 + a_{c0}^2 + 3(a_{w0}^-)^2] + 8(1-\mu^2)\,V_{A0}^2\}/V_{A0}^2, \\ \mathscr{N} &= \{648[V_{A0}^2 + a_{c0}^2 + 3(a_{w0}^-)^2] + 976(1-\mu^2)\,V_{A0}^2 - 675\mu^2\,V_{A0}^2\}/V_{A0}^2. \end{aligned}\right\} \tag{24}$$

Note that $V_p = -\frac{1}{2}\mu V_{A0}$ is the slower of the backward-propagating slow magneto-acoustic modes. (This can be demonstrated from figure 1, where the solid and dashed lines touch each other at $V_p = -\frac{1}{2}\mu V_{A0}$.)

These asymptotic results seem to suggest the system is unstable in general, and the unstable mode is the slower of the backward-propagating slow modes. However, when using a computer to explore the parameter space, we found that the slower mode is not necessarily the unstable one (see §4). Nevertheless, we are confident that the system is unstable almost everywhere, and there is *only one* unstable mode. In particular, it is one of the backward-propagating slow modes (of course, it will be one of the forward-propagating slow modes if we take $P_{w0}^- = 0$ and $P_{w0}^+ \neq 0$ at the outset). Moreover, in most of the parameter space the unstable mode is the slower of the slow modes (see §4).

4. Growth rates

The asymptotic analysis in §3 indicates that the cosmic-ray–plasma system is stable only in exceptional cases. Furthermore, only one of the five magneto-acoustic modes is unstable. These features are confirmed by numerical exploration of the parameter space, taking account of the pressures of plasma, cosmic rays and Alfvén waves, the strength of the magnetic field, the angle between the magnetic field and the direction of propagation of the perturbation, the wavelength of the perturbation, and the coupling between cosmic rays and plasma. To facilitate discussion, we introduce several dimensionless quantities. We recall the *projection factor* $\mu\,(=\mathbf{V}_{A0}.\mathbf{k}/V_{A0}k)$ and the normalized diffusion coefficient $\eta\,(=kl_D$, which mingles the coupling αP_{w0}^- and the wavenumber k; see (15)). The various pressures are represented by the Alfvén Mach number of their 'sound' speeds (McKenzie & Webb 1984; Zank 1989*a*):

$$\beta_{s0} = \frac{a_{s0}^2}{V_{A0}^2}, \quad \beta_{c0} = \frac{a_{c0}^2}{V_{A0}^2}, \quad \beta_{w0}^- = \frac{(a_{w0}^-)^2}{V_{A0}^2}. \tag{25}$$

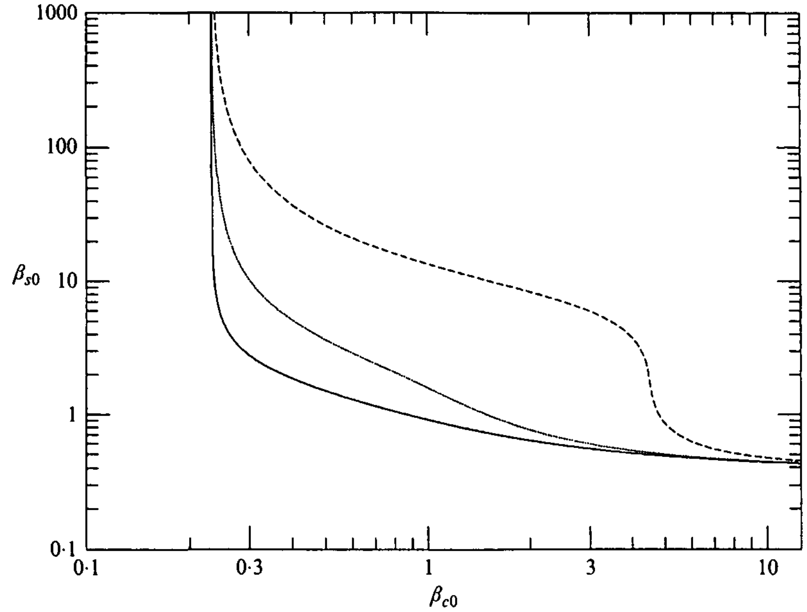

FIGURE 2. The unstable mode is the slow magneto-acoustic mode ($|\mathrm{Re}\,(\omega/V_{A0}\,k)| < \mu$). The solid, dotted and dashed lines correspond to $\eta = 0{\cdot}01$, 1 and 3 respectively. In the region above and to the right of each dividing line, the unstable mode is the faster of the two slow modes (i.e. the one with larger $|\mathrm{Re}\,(\omega)|$), while in the region below and to the left of each line the unstable mode is the slower one. In this example $\beta^-_{w0} = 0{\cdot}1$ and $\mu = 3^{\frac{1}{2}}/2$.

Accordingly, we may take $1/V_{A0}\,k$ as the corresponding time scale. However, if we want to study the growth rates of different perturbation length scales, $1/\nu_-$ (the collision time) or $l_D/V_{A0} = \kappa/V^2_{A0} = c^2/3V^2_{A0}\,\nu_-$ is more appropriate. We tentatively call l_D/V_{A0} the *diffusion time scale*. We define two dimensionless growth rates:

$$\Gamma_k \equiv \mathrm{Im}\left(\frac{\omega}{V_{A0}\,k}\right) = \mathrm{Im}\,(M_p), \quad \Gamma_D \equiv \mathrm{Im}\left(\frac{\omega l_D}{V_{A0}}\right) = \eta\,\mathrm{Im}\,(M_p), \tag{26}$$

where M_p is the Alfvén Mach number of the phase speed V_p of the perturbation.

The expression in square brackets in (13) is the dispersion relation of the magneto-acoustic mode of the cosmic-ray–plasma system. In general, the relation has five complex roots, and a positive imaginary part implies that the corresponding mode is unstable (except when $\eta = 0$, in which case the system may be marginally stable). We searched the parameter space quite extensively and found that, except for a set of measure zero (see §3), the system is unstable, and *one* and *only one* of the roots of the dispersion relation has positive imaginary part. Moreover, this unstable mode is one of the two backward-propagating *slow* magneto-acoustic modes ($-\mu < \mathrm{Re}\,(M_p) < 0$). (Of course, if we have $P^-_{w0} = 0$ while $P^+_{w0} \neq 0$, the unstable mode is the forward-propagating one.)

Each line in figure 2 separates the parameter space into two regions. In the upper/lower region the unstable mode is the faster/slower one (the one with larger/smaller $|\mathrm{Re}\,(M_p)|$) of the slow modes. It is also clear from figure 2 that as

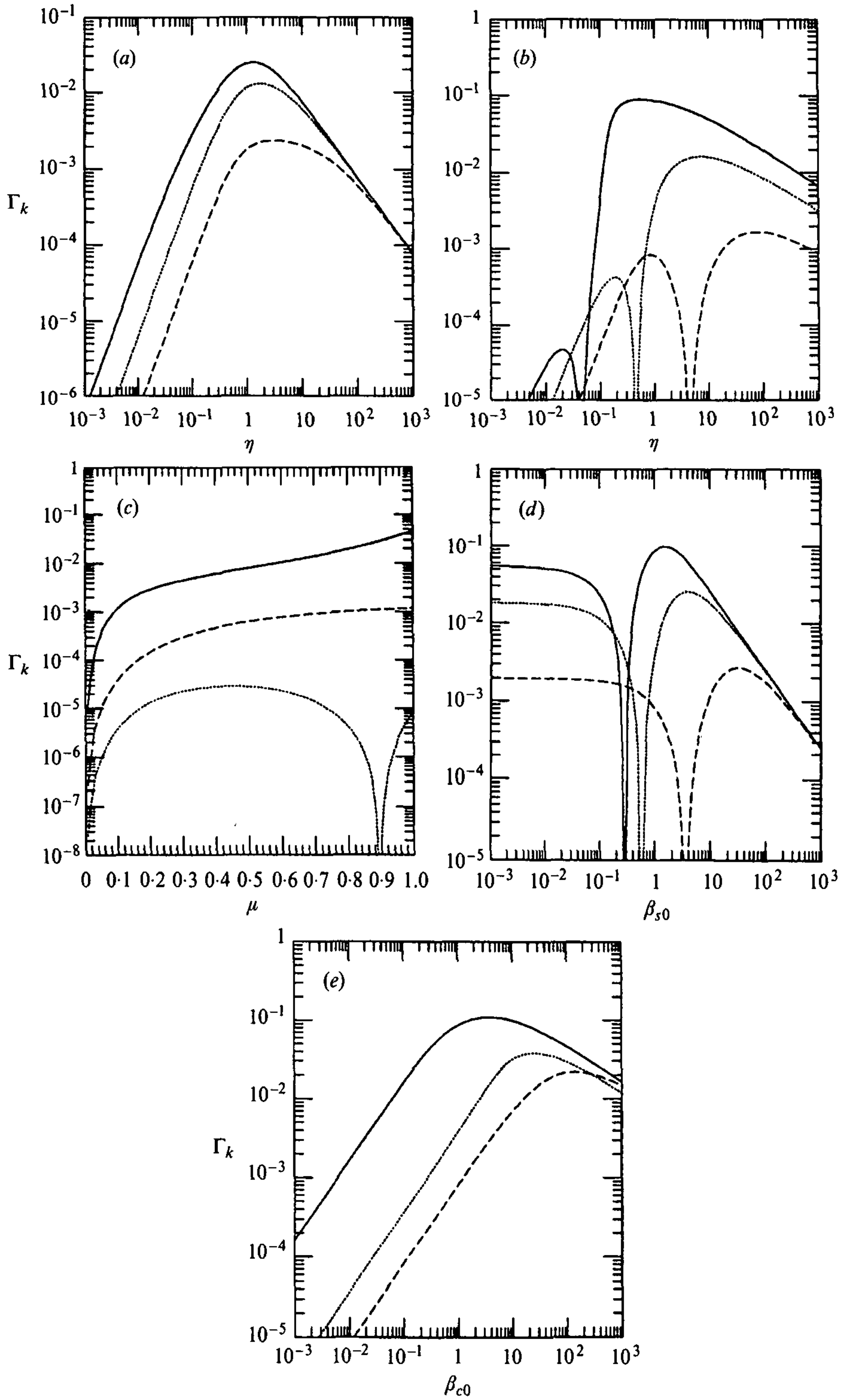

FIGURE 3. The growth rate Γ_k (which is normalized to $V_{A0}k$) as a function of various parameters. The solid, dotted and dashed lines correspond to $\eta\beta_{w0}^{-} = 0{\cdot}1$, 1 and 10 respectively. (*a*) $\beta_{s0} = 0{\cdot}1$, $\beta_{c0} = 1$, $\mu = 1$; (*b*) $\beta_{s0} = 1$, $\beta_{c0} = 1$, $\mu = 1$; (*c*) $\beta_{s0} = 0{\cdot}6$, $\beta_{c0} = 1$, $\eta = 1$; (*d*) $\eta = 1$, $\mu = 1$, $\beta_{c0} = 1$; (*e*) $\eta = 1$, $\mu = 1$, $\beta_{s0} = 1$. The gaps in (*b*)–(*d*) correspond to the condition (16).

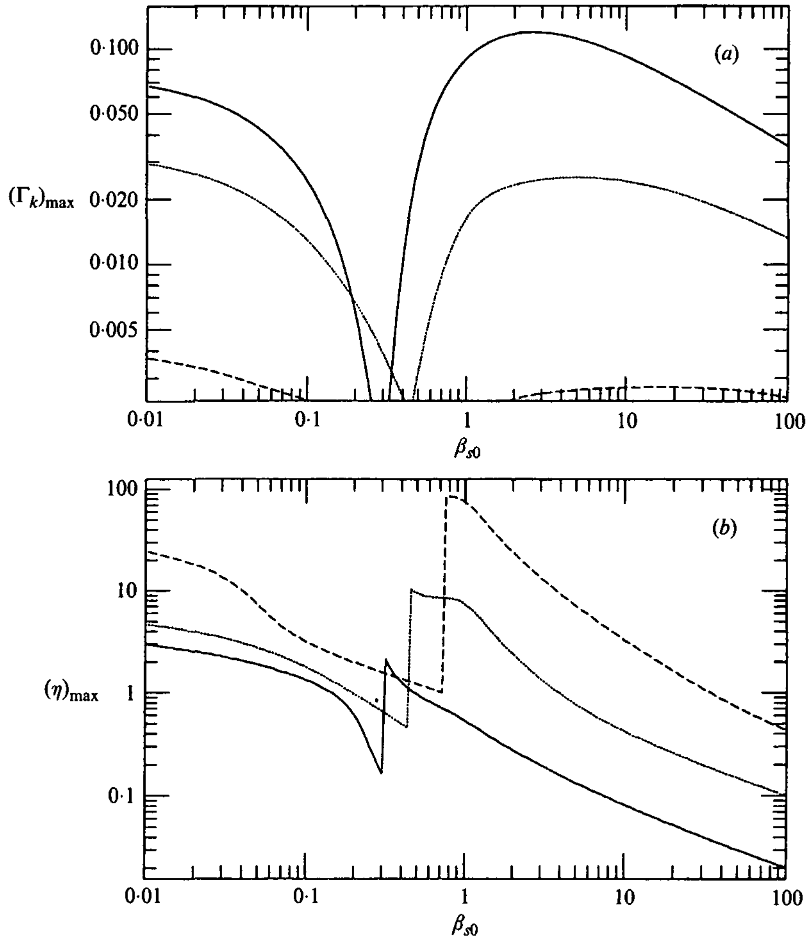

FIGURE 4. (a) $(\Gamma_k)_{\max}$, the maximum of Γ_k with respect to η, versus β_{s0}. (b) $(\eta)_{\max}$, the value of η at which Γ_k is a maximum, versus β_{s0}. The solid, dotted and dashed lines correspond to $\eta\beta_{w0}^{-} = 0{\cdot}1$, 1 and 10 respectively. In this example $\beta_{c0} = 1$ and $\mu = 1$.

η increases, the region for the faster mode shrinks. Hence we confirm the claim that in most of the parameter space the unstable mode is the slower of the slow modes.

We now present two sets of results on the growth rates. In the first we consider Γ_k; thus $V_{A0}k$ is kept fixed and changing η corresponds to changing l_D (or simply P_{w0}^{-}). In the second we consider Γ_D; thus l_D/V_{A0} is kept fixed and changing η corresponds to changing k. (Note that V_{A0} is always kept constant, since it is the normalization for other speeds.) Figures 3(a, b) show that when $\eta = 0$ (or $P_{w0}^{-} \to \infty$), Γ_k vanishes. In some cases (figure 3a), as η increases (or P_{w0}^{-} decreases), Γ_k goes through a maximum and then tends to zero as $\eta \to \infty$ (or $P_{w0}^{-} = 0$). In other cases (figure 3b), Γ_k goes through a maximum first, then drops to zero and rises again to another maximum, and then tends to zero as $\eta \to \infty$. We should point out that the diffusion coefficient is treated as a constant in McKenzie & Webb (1984) and Zank (1989a). They showed that for large enough P_{g0} the system is unstable (they mean $\mathrm{Im}\,(V_p) > 0$) in the long-wavelength limit ($\eta = 0$). In our case the diffusion length scale l_D is inversely

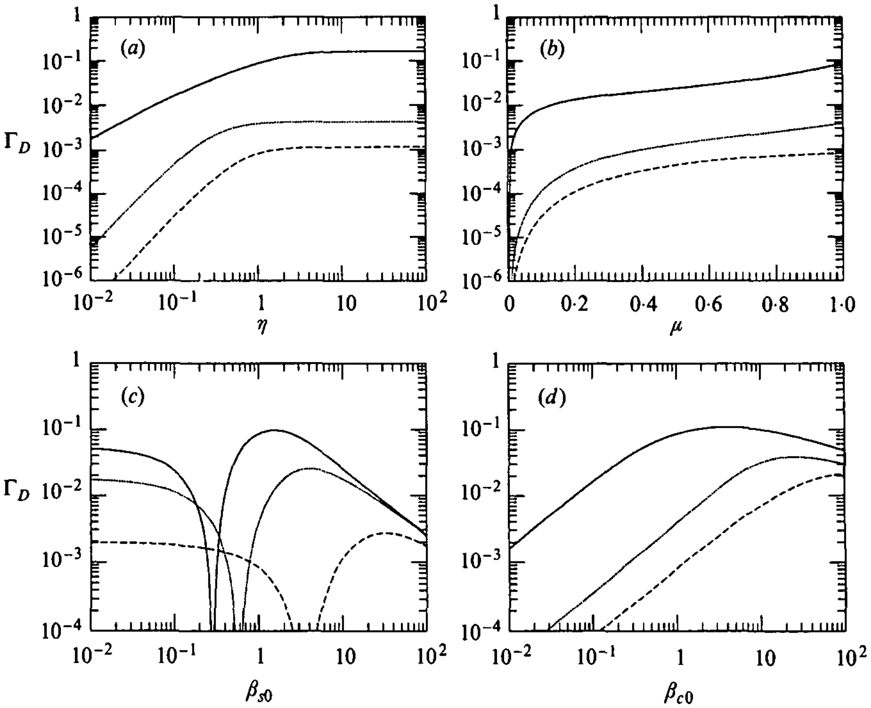

FIGURE 5. Growth rate Γ_D (which is normalized to V_{A0}/l_D) plotted as a function of various parameters. In this figure the solid, dotted and dashed lines correspond to $\beta^-_{w0} = 0{\cdot}1$, 1 and 10 respectively. (*a*) $\beta_{s0} = 1$, $\beta_{c0} = 1$, $\mu = 1$; (*b*) $\beta_{s0} = 1$, $\beta_{c0} = 1$, $\eta = 1$; (*c*) $\eta = 1$, $\mu = 1$, $\beta_{c0} = 1$; (*d*) $\eta = 1$, $\mu = 1$, $\beta_{s0} = 1$. The gaps in (*c*) correspond to the condition (16).

proportional to P^-_{w0}, and the general trend of increasing P^-_{w0} is to stabilize the system. Hence, as η tends to zero, the system becomes less and less unstable, which is in contrast to their result. (Of course, we must remember that the model on which all these analyses based is invalid when the wave pressure becomes too large. Thus letting β^-_{w0} tend to infinity is just for the sake of argument. Moreover, if we keep k and P^-_{w0} fixed and let α tend to infinity, we recover the result of McKenzie & Webb (1984). Nevertheless, we should like to keep α as a constant throughout this paper.) The *gaps* in figures 3(*b–d*) correspond to the stability condition (16). In figure 4 $(\Gamma_k)_{\max}$ is the maximum of Γ_k with respect to η (or equivalently P^-_{w0}), and $(\eta)_{\max}$ is the η at which Γ_k is a maximum. Note that there is a discontinuity in $(\eta)_{\max}$ when β_{s0} satisfies the stability condition (16) (see figure 4*b*).

Figure 5 shows the behaviour of the growth rate Γ_D when the diffusion (or coupling) length scale l_D (i.e. αP^-_{w0}) is kept fixed. Figure 5(*a*) illustrates once again that the growth rate is zero when $\eta = 0$. This simply comes from $k = 0$ (the long-wavelength limit). Γ_D increases monotonically with η (i.e. k), and approaches a constant value $(\Gamma_D)_\infty$ as $\eta \to \infty$ (the short-wavelength limit). This maximum value can be written down explicitly (see (21)):

$$(\Gamma_D)_\infty = a_{c0}^2 \frac{(V_p^{(0)} + \frac{1}{2}\mu V_{A0})^2}{\mu^2 V_{A0}(V_p^{(0)} + \mu V_{A0})} \Big/ \left. \frac{d\mathcal{F}}{dV_p} \right|_{V_p^{(0)}}, \tag{27}$$

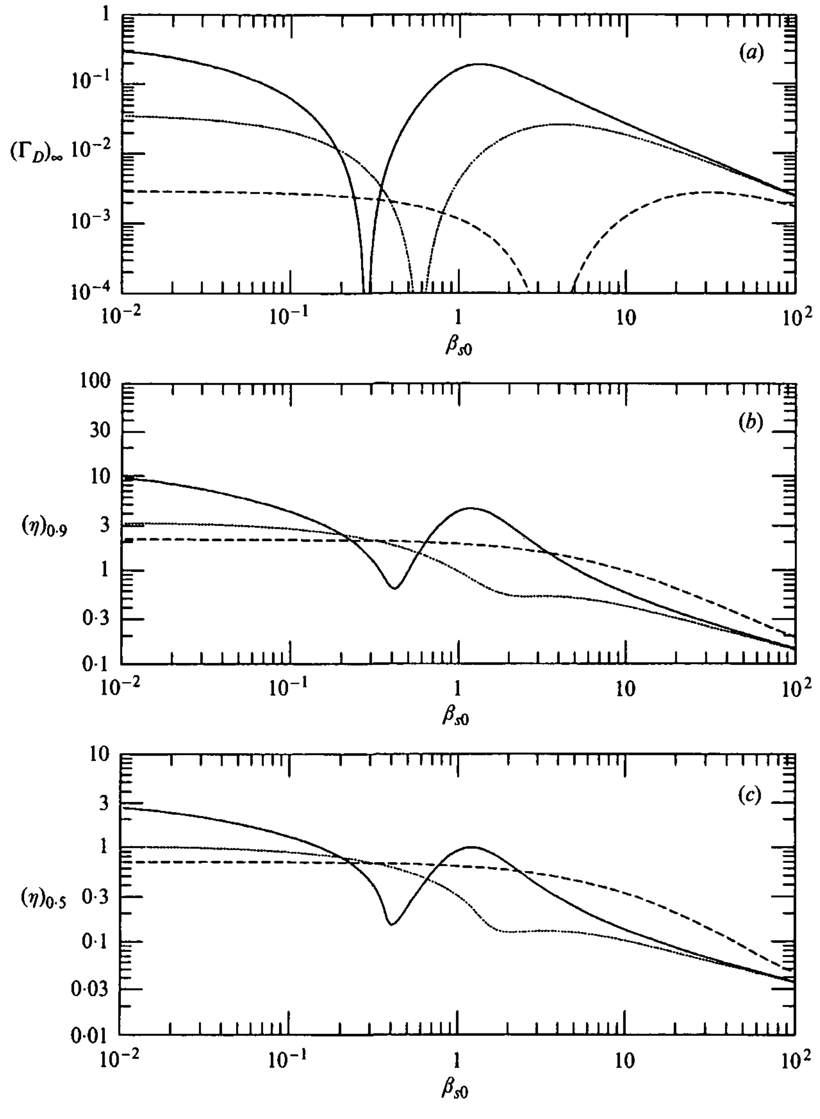

FIGURE 6. (*a*) $(\Gamma_D)_\infty$, the value of Γ_D as $\eta \to \infty$ and given by (27), versus β_{s0}. $(\Gamma_D)_\infty$ is also the maximum of Γ_D with respect to η. (*b*) and (*c*) $(\eta)_{0\cdot9}$ and $(\eta)_{0\cdot5}$, the values of η when $\Gamma_D/(\Gamma_D)_\infty = 0\cdot9$ and $0\cdot5$ respectively, versus β_{s0}. The solid, dotted and dashed lines correspond to $\beta_{w0}^{-} = 0\cdot1$, 1 and 10 respectively. In this example $\beta_{c0} = 1$ and $\mu = 1$.

where $\mathscr{F}$ is given by (18) and $\mathscr{F}(V_p^{(0)}) = 0$. Note that McKenzie & Webb (1984) and Zank (1989*a*) concluded that the system is stable in the short-wavelength limit, because they discussed Im $(\omega/V_{A0}k)$ instead of Im (ω) itself. Here we have Im $(\omega) = \Gamma_D V_{A0}/l_D$. Keeping l_D constant and letting $\eta = kl_D$ tend to infinity gives a finite positive Im (ω). Hence the system is unstable, indeed the *most* unstable, in the short-wavelength limit. The *gaps* in figure 5(*c*) come from the stability condition (16). Figure 5 shows that when the perturbation has length scales smaller than some critical scale, the system becomes *very* unstable. To fix ideas, we define, quite arbitrarily, two length scales $(\eta)_{0\cdot9}$ and $(\eta)_{0\cdot5}$ as the values of η when $\Gamma_D/(\Gamma_D)_\infty = 0{\cdot}9$ and $0{\cdot}5$ respectively. Figure 6 shows how $(\Gamma_D)_\infty$, $(\eta)_{0{\cdot}9}$ and $(\eta)_{0{\cdot}5}$ depend on β_{s0}. These figures are of particular interest in astrophysics, since they give the major unstable length scales of the perturbation. We elaborate on this further in §5.

Finally, numerical results show that the general trend of decreasing μ is to reduce the growth rate (except for the small range around the stability condition (16); see e.g. figure 3*c*), i.e. to stabilize the system.

5. Summary and discussion

The instability of a system consisting of magnetized plasma, cosmic rays and self-excited Alfvén waves has been investigated using a hydrodynamic description of cosmic-ray propagation (Ko 1992). We have re-visited the cosmic-ray-driven magneto-acoustic instability discussed by McKenzie & Webb (1984) and Zank (1989*a*). We have considered a unidirectional wave background (e.g. $P^-_{w0} \neq 0$ and $P^+_{w0} = 0$). The second-order Fermi effect causes the perturbed oppositely directed wave (δP^+_w) to decay, but contributes nothing to the magneto-acoustic instability (recall the dispersion relation (13)). We have taken into account the dependence of the cosmic-ray diffusion coefficient on wave pressure, and hence deduced that the cosmic-ray–plasma system is unconditionally stable in the long-wavelength limit ($\eta = 0$), which is in contrast to the results of McKenzie & Webb (1984) and Zank (1989*a*) (see §4 and figures 3*a*, *b*). However, this is not very important, since we knew from asymptotic analysis (see also Zank 1989*a*) and a numerical search that the system is unstable in almost all circumstances, and the stable region mentioned here is exceptional. The other stable regions are the short-wavelength limit ($kl_D \rightarrow \infty$ with k fixed) and that where the condition (16) is satisfied. (Note that if we take the short-wavelength limit as $kl_D \rightarrow \infty$ with l_D fixed then the system is unstable, in fact, the *most* unstable.) The source of free energy that fuels the instability comes from cosmic rays, and the energy is released through the *frictional* force in generating Alfvén waves when the cosmic rays stream through the magnetized plasma (for a detailed discussion see McKenzie & Webb 1984).

A closer look at figure 4 reveals that when the length scale of the perturbation, k, is fixed, $(\Gamma_k)_{\max}$ (the maximum of the growth rate with respect to η when $V_{A0}k$ is fixed) attains its own *maximum* when $\beta^-_{w0} \lesssim 0{\cdot}5$ and $\beta_{s0} \approx 1$. A similar conclusion can be drawn when the growth rate is normalized to the collisional frequency, $\nu_- = \alpha P^-_{w0}$. Figure 6(*a*) shows that the largest of the local maxima of $(\Gamma_D)_\infty$ (the maximum of the growth rate for fixed αP^-_{w0} occurs when $\eta \rightarrow \infty$) occurs when $\beta_{s0} \approx 1$ and β^-_{w0} is very small. Indeed, analysis shows that for $\mu = 1$ and a given β^-_{w0}, $(\Gamma_D)_\infty$ reaches its local maximum

$$[(\Gamma_D)_\infty]_{\max}$$

$$= -\frac{\beta_{c0}}{8\beta^-_{w0}} \frac{\{[7+36\beta^-_{w0}+48(\beta^-_{w0})^2]\,\beta^-_{w0}-[3+28\beta^-_{w0}+48(\beta^-_{w0})^2][\tfrac{1}{3}\beta^-_{w0}+(\beta^{-2}_{w0})]^{\frac{1}{2}}\}}{\{[2+9\beta^-_{w0}+12(\beta^-_{w0})^2]-(7+12\beta^-_{w0})[\tfrac{1}{3}\beta^-_{w0}+(\beta^{-2}_{w0})]^{\frac{1}{2}}\}}, \tag{28}$$

at

$$\beta_{s0} = 1+\tfrac{10}{3}\beta^-_{w0}+2\beta^{-2}_{w0}-2\beta^-_{w0}[\tfrac{1}{3}\beta^-_{w0}+(\beta^-_{w0})^2]^{\frac{1}{2}}. \tag{29}$$

This maximum is a monotonically decreasing function of β^-_{w0}. When β^-_{w0} tends

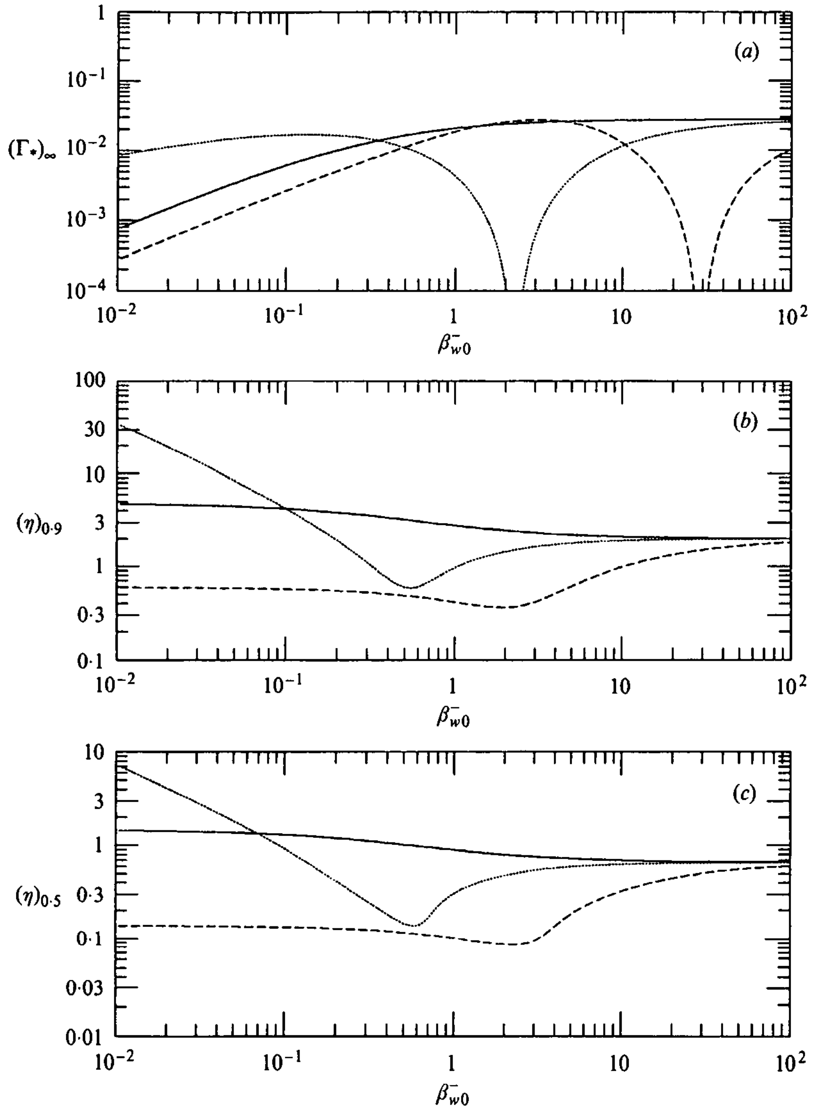

FIGURE 7. (*a*) $(\Gamma_*)_\infty$, the value of Γ_* as $\eta \to \infty$ (which is the maximum of Γ_* with respect to η) versus β^-_{w0}. (*b*) and (*c*) $(\eta)_{0\cdot9}$ and $(\eta)_{0\cdot5}$, the values of η when $\Gamma_*/(\Gamma_*)_\infty = 0\cdot9$ and 0·5 respectively, versus β^-_{w0}. The solid, dotted and dashed lines correspond to $\beta_{s0} = 0\cdot1$, 1 and 10 respectively. In this example, $\beta_{c0} = 1$ and $\mu = 1$.

to zero, the maximum is proportional to $(\beta^-_{w0})^{-\frac{1}{2}}$ and β_{s0} tends to 1. With regard to this, we should make two remarks: (i) we cannot set β^-_{w0} equal to zero, because it is part of the normalization of the growth rate; and (ii) the absolute maximum of $(\Gamma_D)_\infty$ is located at $\beta_{s0} = 0$. To simultaneously explore the relation between the growth rate, the perturbation length scale and the wave pressure, we may introduce another dimensionless growth rate

$$\Gamma_* \equiv \mathrm{Im}\left(\frac{\omega}{2\alpha\rho_0 V_{A0}^4/c^2}\right) = \beta^-_{w0}\,\Gamma_D = \eta\beta^-_{w0}\,\Gamma_k. \tag{30}$$

(However, the time scale $c^2/2\alpha\rho_0 V_{A0}^4$ is rather artificial.) Figure 7 (*a*) shows that for $\beta_{s0} = 1$, $(\Gamma_*)_\infty$ has a maximum at $\beta_{w0}^{-} \approx 0{\cdot}2$. (Note that $(\Gamma*)_\infty \rightarrow \frac{1}{36}\beta_{c0}$ as $\beta_{w0}^{-} \rightarrow \infty$.) After going through all these exercises, we conclude that when $\beta_{s0} \approx 1$ and β_{w0}^{-} is small, the system is *very* unstable. In other words, the cosmic-ray–plasma system is *very* unstable when some kind of *equipartition* occurs between the thermal plasma and magnetic field. Interesting enough, it is generally believed that such equipartition does happen in our Galaxy.

The final outcome of this instability cannot, of course, be determined using the linear analysis presented in this paper. Numerical studies of the full system are therefore desirable. In any event, we can estimate the most unstable length scales, say, in our Galaxy. Following Ptuskin (1981), we take the large-scale magnetic field in our Galaxy as 3×10^{-6} G, and the gas number density as $0{\cdot}1$ cm^{-3} (the warm intercloud region with temperature 10^4 K). The Alfvén speed is then 2×10^6 cm s^{-1}. The cosmic-ray diffusion coefficient in our Galaxy can be estimated by the abundances of secondary nuclei (e.g. Be and B) and the electron component (see e.g. the chapters Ptuskin and Dogiel in Berezinskiĭ *et al.* 1990). A typical value is 10^{28} cm^2 s^{-1}. Therefore the diffusion length scale is about 10^{22} cm. Now, as mentioned above, the cosmic-ray–plasma system is very unstable when $\beta_{s0} \approx 1$ and β_{w0}^{-} is small (say 0·1–0·2). We can read off the *most* unstable length scales from figures 6 and 7. We concentrate on the more *conservative* estimate, $(\eta)_{0{\cdot}9}$. With the above parameters, figures 6 (*b*) and 7 (*b*) give $(\eta)_{0{\cdot}9} \approx 4$. In other words, in our Galaxy the *most* unstable length scales of the cosmic-ray-driven magneto-acoustic instability are those smaller than $\lambda = 2\pi l_D/(\eta)_{0{\cdot}9} \approx 2{\cdot}5$ kpc. The growth time is about $4 \times 10^8/\beta_{c0}$ yr (figure 6*a*). We may take $\beta_{c0} \approx 1$ in our Galaxy. McIvor (1977) showed that short-wavelength hydromagnetic waves can be damped efficiently by thermal conductivity, viscosity and ion–neutral collisions. In the above interstellar medium phase (i.e. the 'hot intercloud regions' in McIvor 1977), all damping rates are $\lesssim 8{\cdot}5 \times 10^{19}(2\pi/\lambda)^2$ s^{-1} (where λ is the wavelength of the waves in cm). Thus for $\lambda \gtrsim 2$ pc dissipation by thermal conductivity, viscosity and ion–neutral collisions cannot suppress the instability described here.

In the case of supernova remnants we take the magnetic field, density and diffusion coefficient as 10^{-5} G, 5×10^{-3} cm^{-3} and 10^{26} cm^2 s^{-1} respectively. The Alfvén speed is 3×10^7 cm s^{-1} and the diffusion length scale is about 3×10^{18} cm. Therefore length scales $\lesssim 1{\cdot}5$ pc are very unstable, and the growth time is about $1{\cdot}5 \times 10^4/\beta_{c0}$ yr.

Finally, we should like to end this paper with two questions. The first is about the stability condition (16). What is so special about the combination of pressures such that the system becomes (marginally) stable, at least in the linear regime? A partial answer may be provided by the fact the component δP_c of the eigenvector of the marginally stable mode vanishes (see (B 2) in appendix B). A natural conclusion is that $\delta P_c = 0$ is a necessary condition for stability. Of course, this does not resolve the puzzle of that specific combination. If the perturbation becomes so large that the linear analysis presented here is no longer valid, will the condition (16) still hold? The second question concerns the evolution of a system containing both forward- and backward-propagating waves. If the system is spatially homogeneous, the second-order Fermi effect drives it towards a unidirectional state (Ko 1992). However, the analysis here shows that this state is unstable to spatial perturbation. So what is the final state?

This work was supported in part by National Science Council, Taiwan, under Grant NSC 82-0208-M-008-102.

Appendix A

In this appendix we give the linearized equations for the general system (cf. McKenzie & Webb 1984):

$$\frac{\partial \delta\rho}{\partial t}+\mathbf{U}_0 . \nabla\delta\rho+\rho_0\nabla . \delta\mathbf{U}+\delta\mathbf{U} . \nabla\rho_0+\delta\rho\nabla . \mathbf{U}_0=0, \tag{A 1}$$

$$\begin{aligned}\frac{\partial \delta\mathbf{U}}{\partial t}+\mathbf{U}_0 . \nabla\,\delta\mathbf{U}+\frac{1}{\rho_0}\nabla(\delta P_g+\delta P_c+\delta P_w^+ +\delta P_w^-)-\frac{1}{\mu_0\rho_0}(\nabla\times\delta\mathbf{B})\times\mathbf{B}_0+\delta\mathbf{U} . \nabla\mathbf{U}_0&\\ +\frac{1}{\mu_0\rho_0}\delta\mathbf{B}\times(\nabla\times\mathbf{B}_0)-\frac{\delta\rho}{\rho_0}\mathbf{g}+\frac{\delta\rho}{\rho_0}\left(\frac{\partial\mathbf{U}_0}{\partial t}+\mathbf{U}_0 . \nabla\mathbf{U}_0\right)&=0,\end{aligned} \tag{A 2}$$

$$\begin{aligned}\frac{\partial \delta P_g}{\partial t}+\mathbf{U}_0 . \nabla\delta P_g-\frac{\gamma_g P_{g0}}{\rho_0}\left(\frac{\partial\delta\rho}{\partial t}+\mathbf{U}_0 . \nabla\delta\rho\right)+\delta\mathbf{U} . \left(\nabla P_{g0}-\frac{\gamma_g P_{g0}}{\rho_0}\nabla\rho_0\right)&\\ -\left(\frac{\delta P_g}{P_{g0}}-\frac{\delta\rho}{\rho_0}\right)\frac{\gamma_g P_{g0}}{\rho_0}\left(\frac{\partial\rho_0}{\partial t}+\mathbf{U}_0 . \nabla\rho_0\right)&=0,\end{aligned} \tag{A 3}$$

$$\begin{aligned}&\frac{\partial \delta P_c}{\partial t}+\left(\mathbf{U}_0+\frac{P_{w0}^+-P_{w0}^-}{P_{w0}^++P_{w0}^-}\mathbf{V}_{A0}\right) . \nabla\delta P_c+\gamma_c P_{c0}\nabla . \left[\delta\mathbf{U}+\frac{P_{w0}^+-P_{w0}^-}{P_{w0}^++P_{w0}^-}\delta\mathbf{V}_A\right.\\ &\quad\left.+\frac{2(P_{w0}^-\delta P_w^+-P_{w0}^+\delta P_w^-)}{(P_{w0}^++P_{w0}^-)^2}\mathbf{V}_{A0}\right]\\ &\quad-\nabla . \left[\frac{c^2}{3\alpha(P_{w0}^++P_{w0}^-)}\frac{\mathbf{V}_{A0}}{V_{A0}}\frac{\mathbf{V}_{A0}}{V_{A0}} . \nabla\delta P_c\right]-16\alpha(\gamma_c-1)\frac{V_{A0}^2}{c^2}\frac{P_{w0}^+P_{w0}^-}{P_{w0}^++P_{w0}^-}\\ &\quad\times\left[\frac{2P_{c0}}{V_{A0}^2}\mathbf{V}_{A0} . \delta\mathbf{V}_A+\frac{P_{w0}^-P_{c0}}{P_{w0}^+(P_{w0}^++P_{w0}^-)}\delta P_w^+ +\frac{P_{w0}^+P_{c0}}{P_{w0}^-(P_{w0}^++P_{w0}^-)}\delta P_w^- +\delta P_c\right]\\ &\quad+\left[\delta\mathbf{U}+\frac{P_{w0}^+-P_{w0}^-}{P_{w0}^++P_{w0}^-}\delta\mathbf{V}_A+\frac{2(P_{w0}^-\delta P_w^+-P_{w0}^+\delta P_w^-)}{(P_{w0}^++P_{w0}^-)^2}\mathbf{V}_{A0}\right] . \nabla P_{c0}\\ &\quad+\gamma_c\delta P_c\nabla . \left[\mathbf{U}_0+\frac{P_{w0}^+-P_{w0}^-}{P_{w0}^++P_{w0}^-}\mathbf{V}_{A0}\right]\\ &\quad+\nabla . \left[\frac{c^2(\delta P_w^++\delta P_w^-)}{3\alpha(P_{w0}^++P_{w0}^-)^2}\frac{\mathbf{V}_{A0}}{V_{A0}}\frac{\mathbf{V}_{A0}}{V_{A0}} . \nabla P_{c0}\right]\\ &\quad-\nabla . \left\{\frac{c^2}{3\alpha(P_{w0}^++P_{w0}^-)}\left[\frac{\mathbf{V}_{A0}}{V_{A0}}\frac{\mathbf{V}_{A0}}{V_{A0}}\times\left(\frac{\delta\mathbf{V}_A}{V_{A0}}\times\frac{\mathbf{V}_{A0}}{V_{A0}}\right)\right.\right.\\ &\quad\left.\left.+\frac{\mathbf{V}_{A0}}{V_{A0}}\times\left(\frac{\delta\mathbf{V}_A}{V_{A0}}\times\frac{\mathbf{V}_{A0}}{V_{A0}}\right)\frac{\mathbf{V}_{A0}}{V_{A0}}\right] . \nabla P_{c0}\right\}=0,\end{aligned} \tag{A 4}$$

$$\begin{aligned}&\frac{\partial \delta P_w^\pm}{\partial t}+(\mathbf{U}_0\pm\mathbf{V}_{A0}) . \nabla\delta P_w^\pm+P_{w0}^\pm\nabla . (\tfrac{3}{2}\delta\mathbf{U}\pm\delta\mathbf{V}_A)\pm\frac{P_{w0}^\pm}{2(P_{w0}^++P_{w0}^-)}\mathbf{V}_{A0} . \nabla\delta P_c\\ &\quad+4\alpha\frac{V_{A0}^2}{c^2}\frac{P_{w0}^+P_{w0}^-}{P_{w0}^++P_{w0}^-}\left[\frac{2P_{c0}}{V_{A0}^2}\mathbf{V}_{A0} . \delta\mathbf{V}_A+\frac{P_{w0}^-P_{c0}}{P_{w0}^+(P_{w0}^++P_{w0}^-)}\delta P_w^+\right.\end{aligned}$$

$$\left.+\frac{P^{+}_{w0}P_{c0}}{P^{-}_{w0}(P^{+}_{w0}+P^{-}_{w0})}\delta P^{-}_{w}+\delta P_{c}\right]+(\delta\mathbf{U}\pm\delta\mathbf{V}_{A}).\nabla P^{\pm}_{w0}+\delta P^{+}_{w}\nabla.(\tfrac{3}{2}\mathbf{U}_{0}\pm\mathbf{V}_{A0})$$

$$\pm\frac{P^{\pm}_{w0}}{2(P^{+}_{w0}+P^{-}_{w0})}\delta\mathbf{V}_{A}.\nabla P_{c0}+\frac{(P^{-}_{w0}\,\delta P^{+}_{w}-P^{+}_{w0}\,\delta P^{-}_{w})}{2(P^{+}_{w0}+P^{-}_{w0})^{2}}\mathbf{V}_{A0}.\nabla P_{c0}=0, \tag{A 5}$$

$$\frac{\partial\delta\mathbf{B}}{\partial t}+\mathbf{U}_{0}.\nabla\delta\mathbf{B}-\mathbf{B}_{0}.\nabla\delta\mathbf{U}+\mathbf{B}_{0}\nabla.\delta\mathbf{U}+\delta\mathbf{U}.\nabla\mathbf{B}_{0}-\delta\mathbf{B}.\nabla\mathbf{U}_{0}+\delta\mathbf{B}\nabla.\mathbf{U}_{0}=0, \tag{A 6}$$

along with the linearized constraint equation

$$\nabla.\delta\mathbf{B}=0, \tag{A 7}$$

and $\delta\mathbf{V}_{A}$ is given by

$$\delta\mathbf{V}_{A}=\frac{\delta\mathbf{B}}{(\mu_{0}\rho_{0})^{\frac{1}{2}}}-\frac{\delta\rho}{2\rho_{0}}\mathbf{V}_{A0}. \tag{A 8}$$

Appendix B

Here we show that the mode represented by the terms in the square-brackets in the dispersion relation (13) is compressive, i.e. $V_{p}^{2}=\delta P_{\text{total}}/\delta\rho$. First we write down some of the components of the eigenvector corresponding to the eigenvalues of the square-bracketted expression in (13):

$$\delta P_{g}=a_{s0}^{2}\,\delta\rho, \tag{B 1}$$

$$\delta P_{c}=a_{c0}^{2}\frac{V_{p}+\frac{1}{2}\mu V_{A0}}{V_{p}+\mu V_{A0}+i\eta\mu^{2}\,V_{A0}}\delta\rho, \tag{B 2}$$

$$\delta P^{-}_{w}=\left[(a^{-}_{w0})^{2}\frac{V_{p}+\frac{1}{3}\mu V_{A0}}{V_{p}+\mu V_{A0}}-a_{c0}^{2}\frac{\frac{1}{2}\mu V_{A0}(V_{p}+\frac{1}{2}\mu V_{A0})}{(V_{p}+\mu V_{A0})(V_{p}+\mu V_{A0}+i\eta\mu^{2}\,V_{A0})}\right]\delta\rho, \tag{B 3}$$

$$V_{A0}.\delta\mathbf{B}=-(\mu_{0}\rho_{0})^{\frac{1}{2}}\frac{\mu V_{A0}}{V_{p}}\mathbf{V}_{A0}.\delta\mathbf{U}+\left(\frac{\mu_{0}}{\rho_{0}}\right)^{\frac{1}{2}}V_{A0}^{2}\,\delta\rho, \tag{B 4}$$

$$\mathbf{V}_{A0}.\delta\mathbf{U}=\left[a_{s0}^{2}+(a^{-}_{w0})^{2}\frac{V_{p}+\frac{1}{3}\mu V_{A0}}{V_{p}+\mu V_{A0}}+a_{c0}^{2}\frac{(V_{p}+\frac{1}{2}\mu V_{A0})^{2}}{(V_{p}+\mu V_{A0})(V_{p}+\mu V_{A0}+i\eta\mu^{2}\,V_{A0})}\right]\frac{\mu V_{A0}}{\rho_{0}\,V_{p}}\delta\rho. \tag{B 5}$$

Recall the linear perturbation of magnetic pressure:

$$\delta P_{B}=\frac{1}{\mu_{0}}\mathbf{B}.\delta\mathbf{B}=\left(\frac{\rho_{0}}{\mu_{0}}\right)^{\frac{1}{2}}\mathbf{V}_{A0}.\delta\mathbf{B}. \tag{B 6}$$

Making use of the square bracketted expression in (13), we obtain the linear perturbation of the total pressure of the system

$$\delta P_{\text{total}}=\delta P_{g}+\delta P_{B}+\delta P_{c}+\delta P^{-}_{w}=V_{p}^{2}\,\delta\rho. \tag{B 7}$$

Thus we have shown that the mode is compressive. Since δP^{+}_{w} does not appear in the square brackets in (13), and in fact it belongs to the decaying mode (the first set of parentheses in (13)); hence it is independent of ρ. Thus we ignore δP^{+}_{w} in the above calculation.

Appendix C

In this appendix we consider a special case to illustrate that the imaginary part of V_{p} is less than or equal to zero when the condition (16) is satisfied. If (16) holds then the square-bracketted expression in the dispersion relation (13) becomes

$$\begin{aligned} 0 = \frac{V_p + \frac{1}{2}\mu V_{A0}}{V_p + \mu V_{A0}} \bigg[& (V_p - \tfrac{1}{2}\mu V_{A0})(V_p + \mu V_{A0}) - \tfrac{4}{3}(a_{w0}^{-})^2 \\ & - a_{c0}^2 \frac{V_p + \frac{1}{2}\mu V_{A0}}{V_p + \mu V_{A0} + i\eta\mu^2 V_{A0}} - \tfrac{4}{3}(1-\mu^2)\, V_{A0}^2 \frac{V_p - \frac{1}{2}\mu V_{A0}}{V_p - \mu V_{A0}} \bigg]. \qquad \text{(C 1)} \end{aligned}$$

Take the simple case $\mu = 1$. The above equation is further reduced to

$$0 = \frac{V_p + \frac{1}{2}V_{A0}}{V_p + V_{A0}} \left[(V_p + V_{A0})(V_p - \tfrac{1}{2}V_{A0}) - \tfrac{4}{3}(a_{w0}^{-})^2 - a_{c0}^2 \frac{V_p + \frac{1}{2}V_{A0}}{V_p + V_{A0} + i\eta V_{A0}} \right]. \qquad \text{(C 2)}$$

The root $V_p = -\frac{1}{2}V_{A0}$ is real, and in the following we show that the remaining three roots have negative imaginary parts. First let $V_p = X + iY$, with real X and Y. The square-bracketted expression in (C 2) becomes two simultaneous equations

$$\begin{aligned} & X^3 + \tfrac{3}{2}V_{A0} X^2 - [3Y^2 + 2\eta V_{A0}\, Y + \tfrac{4}{3}(a_{w0}^{-})^2 + a_{c0}^2]\, X \\ & \qquad - [\tfrac{3}{2}Y^2 + \tfrac{1}{2}\eta V_{A0}\, Y + \tfrac{1}{2}V_{A0}^2 + \tfrac{4}{3}(a_{w0}^{-})^2 + \tfrac{1}{2}a_{c0}^2]\, V_{A0} = 0, \qquad \text{(C 3)} \\ & (3Y + \eta V_{A0}) X^2 + (3Y + \tfrac{1}{2}\eta V_{A0})\, V_{A0} X \\ & \qquad - \{Y^3 + \eta V_{A0}\, Y^2 + [\tfrac{4}{3}(a_{w0}^{-})^2 + a_{c0}^2]\, Y + \eta V_{A0}[\tfrac{1}{2}V_{A0}^2 + \tfrac{4}{3}(a_{w0}^{-})^2]\} = 0. \qquad \text{(C 4)} \end{aligned}$$

Eliminating X from these equations, we obtain a horrendously complication equation for Y:

$$\begin{aligned} 0 = {} & (3Y + \eta V_{A0})\{27\,648 Y^9 + 82\,944 \eta V_{A0}\, Y^8 \\ & + 3456(12a_{c0}^2 + 16(a_{w0}^{-})^2 + 9V_{A0}^2 + 28\eta^2 V_{A0}^2)\, Y^7 \\ & + 576\eta V_{A0}(156a_{c0}^2 + 256(a_{w0}^{-})^2 + 135V_{A0}^2 + 96\eta^2 V_{A0}^2)\, Y^6 \\ & + 108[(12a_{c0}^2 + 16(a_{w0}^{-})^2 + 9V_{A0}^2)^2 \\ & + 4\eta^2 V_{A0}^2(168a_{c0}^2 + 352(a_{w0}^{-})^2 + 171V_{A0}^2) + 144\eta^4 V_{A0}^4]\, Y^5 \\ & + 24\eta V_{A0}[16(3a_{c0}^2 + 4(a_{w0}^{-})^2)(21a_{c0}^2 + 34(a_{w0}^{-})^2) \\ & + 324V_{A0}^2(5a_{c0}^2 + 8(a_{w0}^{-})^2) + 729V_{A0}^4 \\ & + 6\eta^2 V_{A0}^2(180a_{c0}^2 + 544(a_{w0}^{-})^2 + 243V_{A0}^2) + 72\eta^4 V_{A0}^4]\, Y^4 \\ & + \{4[16(3a_{c0}^2 + 4(a_{w0}^{-})^2)^3 \\ & + 108(9a_{c0}^4 + 24a_{c0}^2(a_{w0}^{-})^2 + 4(a_{w0}^{-})^4)\, V_{A0}^2 + 729a_{c0}^2\, V_{A0}^4] \\ & + 3\eta^2 V_{A0}^2[16(261a_{c0}^4 + 1008a_{c0}^2(a_{w0}^{-})^2 + 640a_{w0}^{-4}) \\ & + 216(37a_{c0}^2 + 60(a_{w0}^{-})^2)\, V_{A0}^2 + 3645V_{A0}^4] \\ & + 108\eta^4 V_{A0}^4(32a_{c0}^2 + 192(a_{w0}^{-})^2 + 81V_{A0}^2)\}\, Y^3 \\ & + \eta V_{A0}\{4[16(3a_{c0}^2 + 4(a_{w0}^{-})^2)^3 \\ & + 108(9a_{c0}^4 + 24a_{c0}^2(a_{w0}^{-})^2 + 4(a_{w0}^{-})^4)\, V_{A0}^2 + 729a_{c0}^2\, V_{A0}^4] \\ & + 3\eta^2 V_{A0}^2[16(45a_{c0}^4 + 336a_{c0}^2(a_{w0}^{-})^2 + 128(a_{w0}^{-})^4) \\ & + 216(11a_{c0}^2 + 12(a_{w0}^{-})^2)\, V_{A0}^2 + 729V_{A0}^4] \\ & + 36\eta^4 V_{A0}^4(64(a_{w0}^{-})^2 + 27V_{A0}^2)\}\, Y^2 \\ & + 3a_{c0}^2\, \eta^2 V_{A0}^2[(12a_{c0}^2 + 16(a_{w0}^{-})^2 + 9V_{A0}^2)(12a_{c0}^2 + 64(a_{w0}^{-})^2 + 27V_{A0}^2) \\ & + 12\eta^2 V_{A0}^2(64(a_{w0}^{-})^2 + 27V_{A0}^2)]\, Y \\ & + 72a_{c0}^4\, \eta^3 V_{A0}^3(8(a_{w0}^{-})^2 + 3V_{A0}^2)]. \qquad \text{(C 5)} \end{aligned}$$

Although this equation looks terribly difficult to deal with, we found that all the coefficients are positive. It is clear that Y must be negative in order to satisfy (C 5). Hence the imaginary parts of all four roots of (C 2) are less than or equal to zero. Thus the system is stable when the condition (16) holds. The one for general μ is orders of magnitude more complicated than (C 5) (it has terms up to Y^{20} instead of Y^9), but the same conclusion can be reached.

REFERENCES

AXFORD, W. I., LEER, E. & MCKENZIE, J. F. 1991 *Astron. Astrophys.* **111**, 317.

BEREZINSKIĬ, V. S., BULANOV, S. V., DOGIEL, V. A., GINZBURG, V. L. & PTUSKIN, V. S. 1990 *Astrophysics of Cosmic Rays*. North-Holland.

BREITSCHWERDT, D., MCKENZIE, J. F. & VÖLK, H. J. 1991 *Astron. Astrophys.* **245**, 79.

BREITSCHWERDT, D., MCKENZIE, J. F. & VÖLK, H. J. 1993 *Astron. Astrophys.* **269**, 54.

DRURY, L. O'C. & VÖLK, H. J. 1981 *Astrophys. J.* **248**, 344.

DRURY, L. O'C., MARKIEWICZ, W. J. & VÖLK, H. J. 1989 *Astron. Astrophys.* **225**, 179.

DUFFY, P. 1992 *Astron. Astrophys.* **262**, 281.

HARTQUIST, T. W. & MORFILL, G. E. 1986 *Astrophys. J.* **311**, 518.

IPAVICH, F. M. 1975 *Astrophys. J.* **196**, 107.

JONES, T. W. & KANG, H. S. 1992 *Astrophys. J.* **396**, 575.

KO, C. M. 1991*a* *Astron. Astrophys.* **242**, 85.

KO, C. M. 1991*b* *Astron. Astrophys.* **251**, 713.

KO, C. M. 1992 *Astron. Astrophys.* **259**, 377.

KO, C. M., DOUGHERTY, M. K. & MCKENZIE, J. F. 1991 *Astron. Astrophys.* **241**, 62.

KO, C. M., JOKIPII, J. R. & WEBB, G. M. 1988 *Astrophys. J.* **326**, 761.

LEE, M. A. & AXFORD, W. I. 1988 *Astron. Astrophys.* **194**, 297.

MCIVOR, I. 1977 *Mon. Not. R. Astron. Soc.* **178**, 85.

MCKENZIE, J. F. & VÖLK, H. J. 1982 *Astron. Astrophys.* **116**, 191.

MCKENZIE, J. F. & WEBB, G. M. 1984 *J. Plasma Phys.* **31**, 275.

PTUSKIN, V. S. 1981 *Astrophys. Space Sci.* **76**, 265.

WEBB, G. M. 1983 *Astron. Astrophys.* **127**, 97.

ZANK, G. P. 1989*a* *J. Plasma Phys.* **41**, 89.

ZANK, G. P. 1989*b* *Astron. Astrophys.* **225**, 37.